

LIGAND BASED PHARMACOPHORE MODELING AND QSAR ANALYSIS OF HETEROCYCLIC DIAMIDINE DERIVATIVES AS ANTI-PARASITIC DNA MINOR GROOVE BINDERS

Subhadip Banerjee¹, Anil Kumar Saikia^{*2}

ABSTRACT: Ligand based pharmacophore modelling (LBPM) of a group of 26 heterocyclic diamidine derivatives having clinical bioactivity against *Trypanosoma brucei gambiense* (TBG). A four point pharmacophore model of anti-parasitic diamidines has been developed. Positive ionic and aromatic features were identified as crucial features for showing bioactivity as DNA binders. A statistically feasible 3D QSAR model was developed for further evaluation of the developed pharmacophore model. The good predictive ability of the model has been examined by various statistical parameters like $Q^2=0.67$, $r^2_{pred}=0.96$ value. This model can be used for *in silico* screening and designing of potent anti-parasitic molecules.

Key word: Anti-parasitic, Diamidine, Pharmacophore, 3D QSAR.

INTRODUCTION

Diseases like trypanosomiasis, leishmaniasis, and malaria are now in an epidemic stage in humans and animals, caused about millions of fatalities due to their transmission across geographical barriers and due to absence of potent drug for treatment (Fairlamb 2003, Bouteille *et al.*, 2003). Moreover emergence of drug resistant species have made the scientific community attached with drug development to search for better options to have more advanced therapeutic edge against the drug resistant species. The phenomenon of drug resistance is almost inevitable and becoming clinically unmanageable. Hence developing anti-parasitic

drug becomes an important aspect for better therapeutic point of view.

Protozoan parasites exhibit a broad range of peculiarity, including polycistronic transcription, trans-splicing of precursor mRNAs which is likely due to the early divergence of the eukaryotic lineage (Yeates 2003). Mitochondrial DNA organization and the RNA controlling process are remarkable features of kinetoplastids, which consists of a single mitochondrion encircling an exclusive type of DNA organization called kinetoplast DNA (kDNA), consisting of thousands of interlocked circular DNA molecules, referred to as minicircles and maxicircles (Estevez and

¹Bengal Institute of Pharmaceutical Sciences, Kalyani, Nadia, Pin-741235, West Bengal, India.

²Department of Pharmaceutical Sciences, Dibrugarh University, Pin-786004, Assam, India.

* Corresponding author.

Simpson 1999, Liu *et al.* 2005). This kinetoplast DNA has been an important target in trypanosomiasis caused by *Trypanosoma cruzi*. DNA minor groove binders show a variety of bioactivity and is a effective strategy in rational drug design (Tidwell and Boykin 2003, Wilson *et al.* 2005).

In the present study, a correlation between anti-parasitic activity with that of structural properties of heterocyclic diamidine has been analyzed employing ligand based pharmacophore model (LBPM) approach. The compounds used in this study possess structural similarity with bioactive, less toxic, orally available pro-drug showing clinical practicability up to phase II (Athri *et al.* 2006, Bailly and Chaires 1998). The 3D pharmacophore alignment based study is especially very important for further quantification of structure activity relationship in the 3D space. Thus it is a very important step towards answering the structural basis of the activity of these molecules.

However, pharmacophore analysis with respect to chemical, structural, topological and other properties provide an outline for designing new compounds. Moreover, the receptor interaction pattern and important features of the same can also be elucidated by this analysis. It is reported that DNA binding is involved in the bioactivity of diamidine derivatives that target infectious disease organisms (Henderson and Hurley 1995, Baraldi *et al.* 2004). The present scenario turns out to be case where the ligands bind to the minor groove of the AT-rich sequence of DNA selectively can change, modify or stop the transcription of a specific enzyme (Cory *et al.* 1992, Wilson *et al.* 1998). In leishmania and trypanosomes, the mitochondrial kineto-plast DNA (kDNA) is the

primary attack zone of diamidine (Shapiro and Englund 1990 and 1995.) The trypanosome kinetoplast, have recurring AT zone sequences form a specific and effective target for heterocyclic diamidines (Athri *et al.* 2006).The pharmacophore based 3D QSAR model will help us to gain insight about the structural requirements for better activity.

For the successful generation of the 3D QSAR model we have used PHASE (Dixon *et al.* 2006) algorithm of Schrodinger molecular modeling suite. A statistically significant 3D QSAR model which may be further used for development of new effective molecules or finding a druggable hit out of a virtual screening process of drug development on the basis of this 3D QSAR model.

MATERIALS AND METHODS

1. Data sets and Biological activity:

26 heterocyclic diamidine derivatives from the literature by Athri *et al.* (2006) were selected. The molecules were selected considering their IC_{50} values to be precise and not in range. The insoluble compounds were discarded. The biological activities taken for study were converted to pIC_{50} values, using Gaussian statistics, the distribution of the activity were shown (Fig.1) to get a more significant figure for visualizing bioactivity. Thus out of 26 heterocyclic diamidine derivatives, 70% compounds were taken as training set and the rest of the compounds were used as a test set. All the 2D molecular structures were developed using Chem Draw Ultra 8.0 and then were transformed into 3D structures. Energy minimization was done using OPLS 2005 force field of Ligprep module. The pH of ionization and other parameters of the molecules were adjusted and calculated from

default settings of aforesaid module. For the development of the pharmacophore model these ligands were imported in PHASE working interface. Conformation generation is an important step in PHASE algorithm; conformations were generated using Configen taking GB/SA solvent treatment model. About 10,000 conformers were generated per structure and ensuing 100 step preprocess and 50 step post process minimization by varying the conformations of amide bonds. The minimized conformers were filtered using a relative energy parameter limitation of 10 kcal mol⁻¹ and a minimum atom deviation of 1.00 Å. If there is any occurrence in which the energy in a conformer is higher than this limit, and then its incessant disposition was ensured. The superfluous conformers were eliminated based on RMSD filter window of 0.5Å for further refinement. Thus we successfully incorporated only the lowest energy conformation of a ligand in the process of pharmacophore model development. A couple of conformer was defined as identical if the distance between them is below 1.00 Å.

2. Creating Pharmacophore Sites and Common pharmacophore hypothesis generation:

According to the pIC₅₀ values the molecules were divided into active and inactive setting the maximum and minimum values in the activity threshold window of PHASE. Pharmacophore sites of a ligand are represented in the 3D space by a set of points. These points coincide with various chemical characteristics with type, location and directionality, which facilitate non covalent bonding with the receptor sites. The pharmacophore features like hydrogen bond acceptor (A), hydrogen bond donor (D),

hydrophobic/Non-polar group (H), negatively ionizable (N), positively ionizable (P) and aromatic ring (R) present in the PHASE were used to create the pharmacophore sites for the energy calculated ligands. The following features were assigned using SMART queries. Tree based partition algorithm is used by PHASE for detection of common pharmacophore from a set of variants taking maximum tree depth 3. To find common pharmacophore PHASE algorithm use an exhaustive analysis of k-point pharmacophore match picked from the conformations of a set of active ligands on the basis of inter site distances, and then find all spatial arrangements of pharmacophore features those are common to at least 8 out of 10 active ligands. Thus the pharmacophores generated have matches across different set of actives eliminating the chance of its exclusiveness towards a small subset of ligands. The different pharmacophore hypothesis produced were further examined by using a scoring function so that it produced the best alignment of the ligands which are active yet also incorporating the features from the inactives to make the model more versatile.

3. Scoring Pharmacophores according to actives and inactives:

The pharmacophore hypotheses were scored pertaining to the active ligands. To ensure that no inappropriate pharmacophore is inside the survived pharmacophore models least squares site-to-site alignment is considered. Now the scoring of the pharmacophore hypotheses was done in relation to the information from the active ligands considering various geometric and heuristic factors. The alignment to a reference pharmacophore is considered according to RMSD of the site points and the

average cosine of the vectors keeping their tolerance 1.2 Å and 0.5 respectively was set. To preferentially get the reference ligand from the most active set the ones scoring the upper 10 % was considered for score calculation. For further refinement volume scoring is also done in order to measure quantitatively of how each non-reference ligand is superimposing with the reference ligand, in account of Vander Waals models of the structures and taking into account all heavy atoms of the active ligands. Here the cutoff for volume scoring was kept at 1.00 for the nonreference pharmacophores. To ensure the lowest energy ligands for better binding to be incorporated in the best pharmacophore the relative conformational energy of the reference ligand was constrained to 0.001. Thus we generated the survival active scores for the pharmacophore hypotheses. A ligand can be inactive due to number of ways but for successful implementation of only those characters which are important for good binding we need to incorporate the knowledge why the inactive molecules are inactive. This would make our pharmacophore models a better one having ability to distinguish between an active and an inactive molecule. This score inactive is calculated with the help of fitness score which is assessed with the same constraints as that of score active. A good hypothesis has a low fitness score multiplied by a user adjustable factor which was set to default mode. For the development of pharmacophore model we considered the highest active molecule 11, 21, 24. The pharmacophore fitness score 3 is the highest score observed for these ligands, which denotes how good a molecule fit with the pharmacophore hypothesis. These fitness score and bioactivity were correlated, when the distance and angle between each feature are

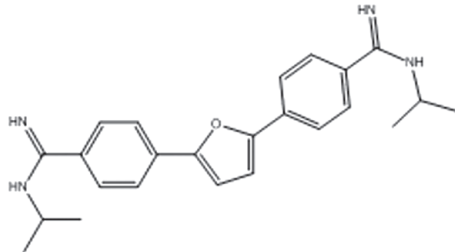
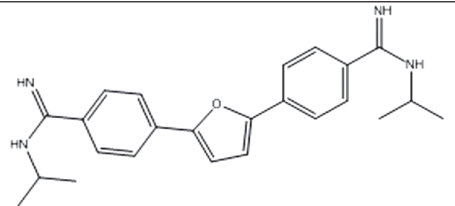
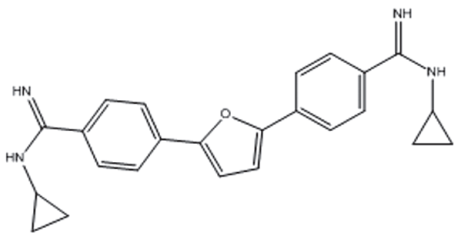
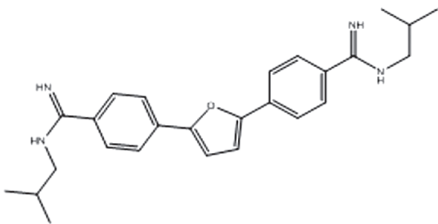
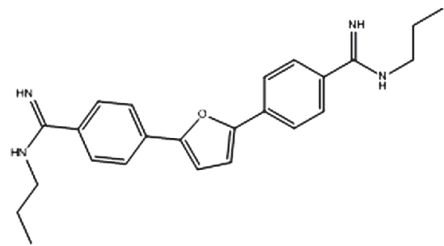
variable, results the generation of ten pharmacophore hypotheses. The ranking is done for these models on the basis of all this said scores, considering the ability to distinguish between active and inactive ligands. The scores are calculated on the basis of contributions from the alignment of site points and vectors, volume overlap, selectivity, number of ligands matched, relative conformational energy, and activity. A common pharmacophore model (CPM) among the group of ten pharmacophore hypotheses were selected according to their maximum active and inactive contribution of features; followed by its fitness and stability based on the smart scoring function. For generation of CPM both active and in-active molecules are taken in consideration for further refinement, such that the generated pharmacophore model had the ability to distinguish between the active and inactive features of molecules.

4. 3D-QSAR model generation:

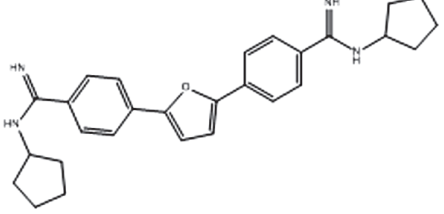
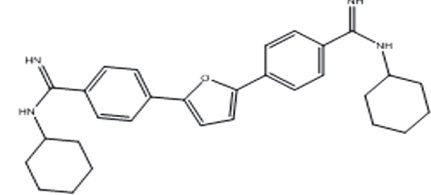
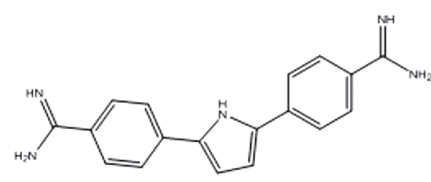
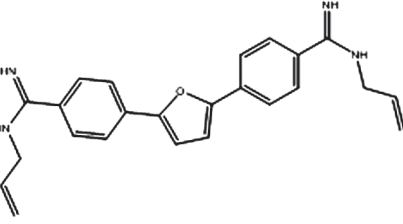
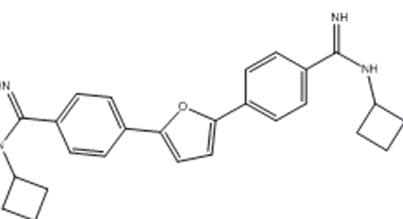
Atom based 3D QSAR model of pharmacophore hypotheses was generated by us. The atom based 3D QSAR model was chosen as our data set ligands showed quite very good alignment as it consisted of a large variety of derivatives of a parent molecule. The atom based 3D QSAR model provides more chemical significance than pharmacophore based 3D QSAR model which only depends upon pharmacophore sites for alignment to the hypothesis selected. This is because of the fact that atom based 3D QSAR takes the total molecule and facts like probable steric hindrance with the receptor site can be taken into account while building a model with this atom based approach.

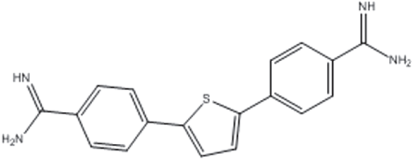
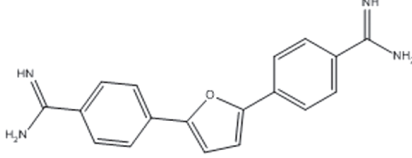
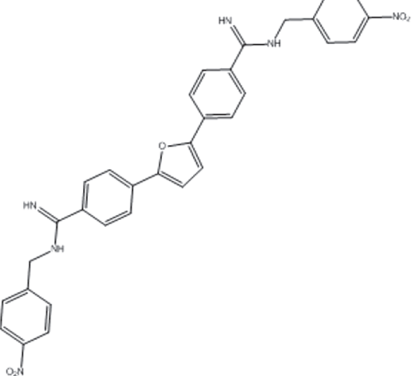
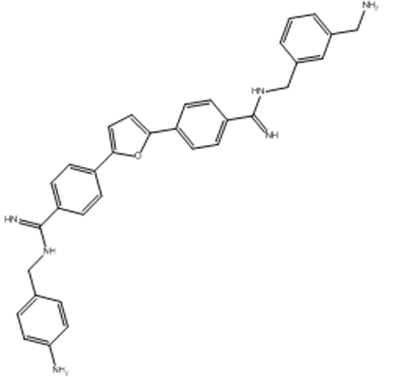
The PHASE algorithm uses a very versatile

Table 1: Training and Test set showing activity, predicted activity and fitness.

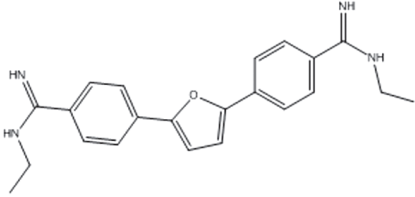
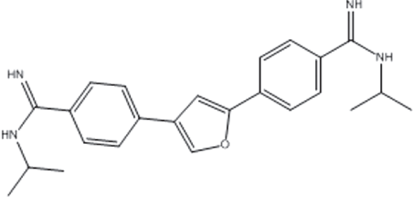
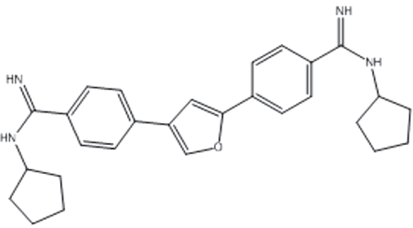
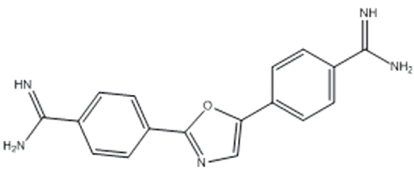
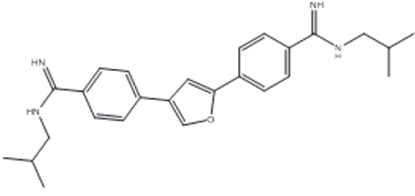
ID	Structure	QSAR Set	PIC ₅₀	Predicted pIC ₅₀	Fitness
1		training	2.29	2.09	2.32
2		training	1.16	1.43	2.33
3		training	1.63	1.92	2.35
4		test	1.45	1.58	2.29
5		test	1.35	1.61	2.33

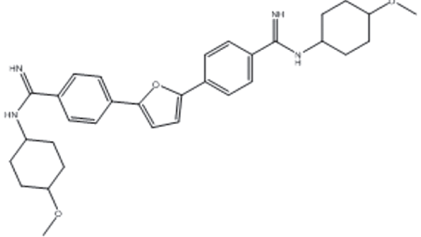
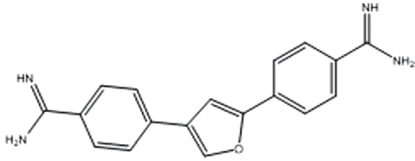
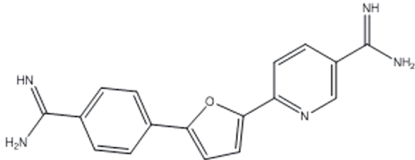
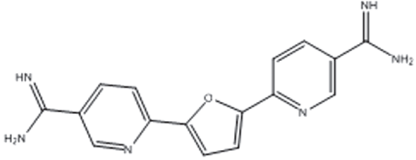
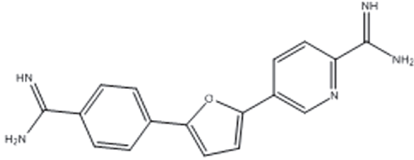
Ligand based pharmacophore modeling and QSAR analysis of heterocyclic diamidine..

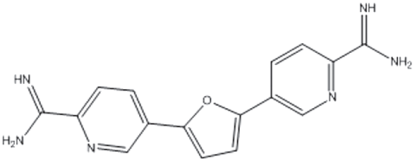
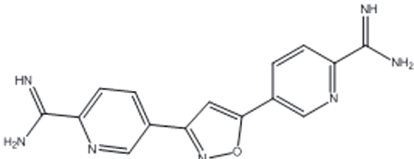
ID	Structure	QSAR Set	PIC ₅₀	Predicted pIC ₅₀	Fitness
6		training	1.45	1.4	2.28
7		training	1.17	1.12	2.15
8		training	1.85	1.96	2.42
9		training	1.63	1.79	2.32
10		training	1.97	1.87	2.31

ID	Structure	QSAR Set	PIC ₅₀	Predicted pIC ₅₀	Fitness
11		test	2.52	2.26	2.67
12		test	2.18	2.13	2.3
13		training	0.99	1.03	2.19
14		training	1.91	1.86	2.21

Ligand based pharmacophore modeling and QSAR analysis of heterocyclic diamidine..

ID	Structure	QSAR Set	PIC ₅₀	Predicted pIC ₅₀	Fitness
15		training	2	1.94	2.38
16		training	1.16	1.16	2.74
17		test	1.72	1.35	2.68
18		training	2.15	2.21	2.39
19		test	1.86	1.78	2.44

ID	Structure	QSAR Set	PIC ₅₀	Predicted pIC ₅₀	Fitness
20		training	0.77	0.68	2.2
21		training	2.77	2.37	3
22		training	2.31	2.25	2.33
23		training	1.77	1.89	2.14
24		test	2.68	2.07	2.51

ID	Structure	QSAR Set	PIC ₅₀	Predicted pIC ₅₀	Fitness
25		training	2.39	2.52	2.34
26		training	2.28	2.28	2.38

approach for the development of 3D QSAR model. It considers a rectangular grid of 1 Å grid distance in a 3D space. Thus it creates cubes of said dimension in the 3D space. The atoms of the molecules which are considered as overlapping Vander Waal spheres fall inside these cubes depending on the volume of the atomic spheres. These occupied cube spaces are termed as volume bits. A volume bit is allocated for each different class of atom that occupies a cube. There are six atom classes two hydrogen bond acceptor (A), one positively ionizable (P) and two aromatic ring (R) used for classifying the atom characteristics. The total number of volume bits consigned to a specified cube is

Table 2: Distance between pharmacophoric features.

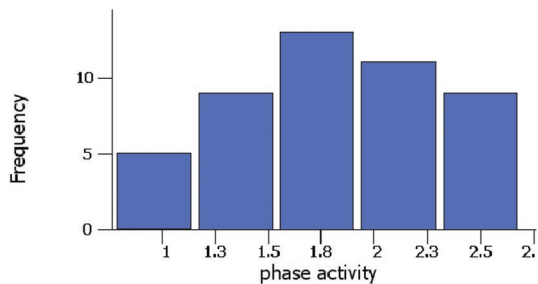
PF1	PF2	Distance
P4	P3	13.995
P4	R6	6.898
P4	R7	2.864
P3	R6	7.759
P3	R7	11.290
R6	R7	4.036

*PF= Pharmacophoric features

Table 3: Statistical result of 3D QSAR model.

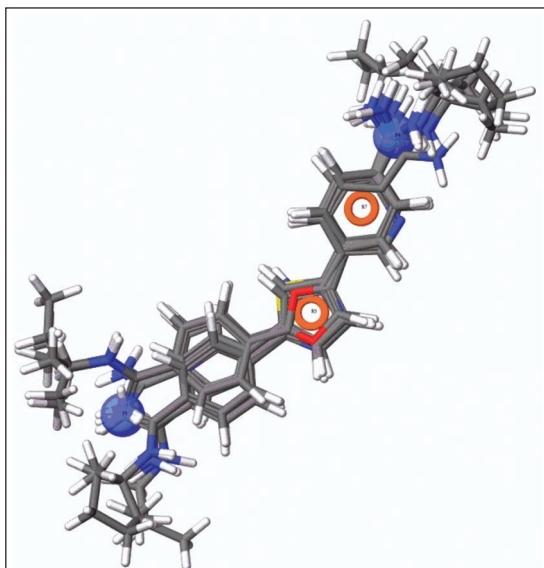
ID	PLS Factor	SD	R ²	RMSE	Q ²	Pearson-R	R ² _{pred}
PPRR.3	3	0.22	0.85	0.3	0.6	0.84	0.955

Fig. 1: Histogram showing activity distribution of the dataset.



based on how many training set molecules occupy that cube. A single cube may represent the occupation by one or various atoms or sites, and even those from the same molecule or may be from unlike molecules of the training set. Thus A molecule may be represented by a binary string concurrent to the occupied cubes, and also the various types of atomic sites that exist in those cubes. To create an Atom based QSAR

Fig. 2: Structural alignment of the data set and pharmacophore.



model, these volume bits which encodes the geometries and chemical characteristics of the molecule are regarded as independent variables in PLS (Partial Least square) regression analysis. For generating a predictive QSAR model we have to select 3 number of PLS factor. The maximum PLS factor that can be taken is $N/5$ where N is the number of ligands present in the training set.

RESULT AND DISCUSSION

In our successful effort to develop a predictive and statistically significant pharmacophore based 3D QSAR model, we selected a pharmacophore hypothesis according to their highest survival active and inactive score that also shows good structural alignment (Fig.2) to the highest active molecules as well as had the ability to align to non model inactive ligands having less value than active threshold set for the model as well. It also illustrated diversified variants ensuring its uniqueness and selectivity. Thus we tried to avoid pharmacophore hypotheses with less variant contribution or less specificity or selectivity in its fingerprint. Out of 10 pharmacophore hypotheses the highest ranking was PPRR.3 (Fig.3) calculated according to the effective

Fig. 3: The pharmacophore hypothesis.

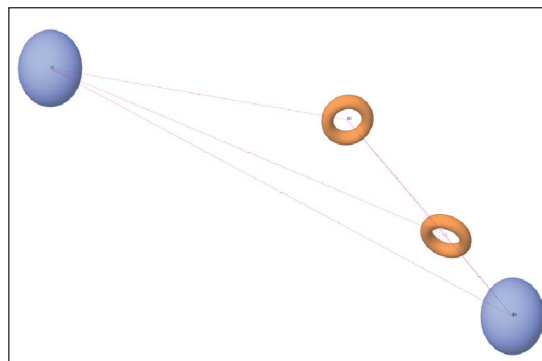
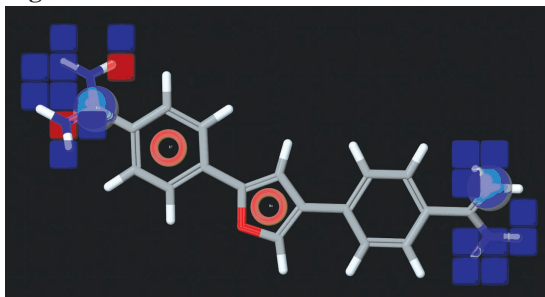


Fig.4: H-Bond donor contribution.



scoring function already described in section 2.3. Thus in the process of scoring and validation based evolution among the pharmacophore alternatives, one got finally selected; it is a four point pharmacophore containing two variants; two positively ionizable (P) groups and two aromatic rings (R). The distance and angle between each pharmacophoric features are summarized in Table 2. This pharmacophore model was further exploited for aligning the ligands used in 3D QSAR model generation.

1. Pharmacophore model

Three compounds with highest activity from the total data set were selected for common pharmacophore hypotheses (CPH) generation. Using a tree-based partition algorithm requiring that all active compounds must match, 16 four featured probable common pharmacophore hypotheses were generated from the list of

Fig. 6: Electron withdrawing contribution.

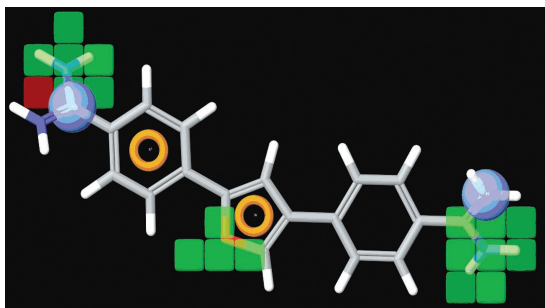
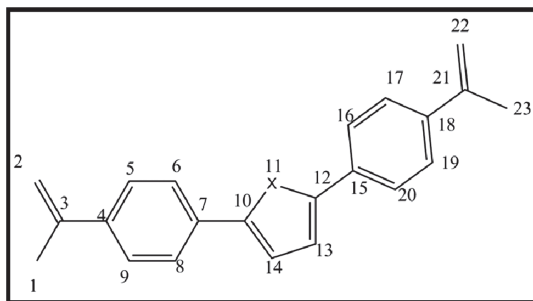


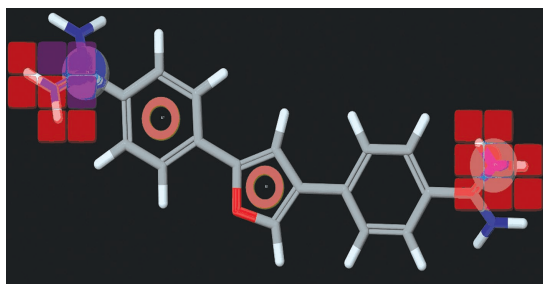
Fig.5: Structure skeleton.



variants. No common pharmacophore hypotheses were obtained for five and six common features. On applying the scoring function for four-featured common pharmacophore hypotheses using default values, 10 common pharmacophore hypotheses survived, belonging to the types PPRR. Training set compounds were aligned on these common pharmacophore hypotheses and analyzed by PLS analysis described in PHASE with ten PLS factors.

A good alignment is the primary requirement for a finer QSAR analysis. However validation is an imperative aspect for QSAR analysis, as a matter of fact diffused distribution of characters and activities amount the training set is a prerogative, 70% of the total ligands were chosen in the training set and the rest was taken in test set (Table 1) based on the activity guided Hierarchical Clustering method for internal validation purpose. The statistical outcomes of

Fig.7: Positive ionic contribution.



the model thus produced indicated its statistical significance and predictive ability. The PLS analysis results of the model thus produced among various hypotheses was the best further justified our selected pharmacophore was the fittest. The various statistical parameters R^2 (Correlation coefficient), Q^2 (q^2 for the predicted activity), SD (Standard Deviation), $RMSE$ (Root mean square error), P (Significance level of variance ratio), F -Statistics, $Pearson-R$ (correlation between the predicted and observed activity of test set), and r^2_{pred} which was calculated from the formula

$$r^2_{pred} = (SD-PRESS)/SD$$

where SD is the sum of the squared differences between the experimental biological activities of the test set ligands and mean of the experimental activities of the training set molecules and $PRESS$ is the sum of squared differences between predicted and actual experimental activity values for every ligand in test set. To avoid over-fitting of the results for PLS factor 3 were used and sum up of these statistical parameters are shown in Table 3.

2. Interpretation of Atom based 3D QSAR model

The ligand based 3D QSAR model out of the selected pharmacophore hypothesis thus produced showed the contributions of various chemical variants or atoms or groups to enhance activity or decrease the activity of ligands. For mapping and visualization of our atom based 3D QSAR model result we interpreted the various physicochemical contributions responsible on the basis of 21 the highest active ligand as the template. Using the map we also correlated our predicted result with that of *in vitro* bioactivity and find the structural and

chemical basis for the activity of other active and inactive ligands under an activity threshold. Here we discussed the various chemical contributions of the ligands according to the model.

i). H-Bond donor contribution:

The color mapping of the ligand according to the model shows the H-bond donor (HBD) contributions (Fig.4). The blue cube regions of the ligands will show favorable contribution and the red cube regions are unfavorable for the contribution of H-bond donor property. That indicates that presence of HBD group like $-NH_2$ will be favorable for showing antitrypanosome bio-activity. Appearance of red color blocks around the $=NH$ group of benzimidamido fragment indicates reduction of this group to $-NH_2$ group may be favorable for bio activity. This is clear from the features attaining from lowest active molecule 20, contain N-(4-methoxycyclohexyl) benzimidamido residue. But in moderately active molecule 14, 26 blue color region come into sight around the $-NH_2$ group of terminal phenylmethanamine and picolinimidamido residue indicates the importance of $-NH_2$ group. Moreover it can be distinctly observed that around position 1 and 2 of skeleton structure (Fig.5) a red cube is also there which refers that if there is a H-bond donor atom it will have negative impact on bioactivity. It may be due to donor-donor field interaction at two hands attached to the position 1 and 2 explaining the fact we see that in compounds 1,11,18,21,22,24,25,26 show high activity due to the presence of a H atom attached to N and no other HBD is present. While in ligands 13, 14 and 20 due the presence of additional H-bond donor like N and O attached to a ring

around 1 and 2 positions show quite decreased activity around 1 or less due the effect of two H-bond donors nullifying each other. Based on this line of evidence it can be concluded that free -NH_2 HBD type of groups are essential to produce superior bioactivity.

ii). Electron withdrawing contribution:

The color map of (Fig.6) shows the contribution of electron withdrawing effect (EWE). The green cubes shows positive or favorable contribution and the red cubes shows negative contribution. The highest activity of the ligand is due to this positive contribution only. It's clearly shown that the ligand is having tight fitting to the green cubes at the pharmacophore points having electron withdrawing groups at those positions contributing for its highest activity. Thus if a ligand can be designed in such a way that the following green regions contain some electron withdrawing group will show high activity. Thus the N atom at positions 1, 2, 22, 23 of (Fig.5) where the green cubes are placed quantify for the bioactivity of all the compounds. The different atoms as electron withdrawing groups at position 11 of the skeleton structure (Fig.5) cause change in the activity. In 1, 2, 21, 22,23,24,25 have O atom at the position show quite an increased activity others like 11 sulphur atom show less activity and 8, 18, 19 having N atom show slightly lower activity as the following groups have weak electron withdrawing contribution comparatively. The red cubes at position 1 of the skeleton explain the decreased activity of the compounds 2,3,4,5,6,7,9,16,19 due to the presence of various electron withdrawing groups at the unfavorable position.

iii). Positive ionic contribution:

The color map (Fig.7) shows the positive ionic contribution of the ligand by the model. The red cubes shows negative contribution and the violet cubes show the positive contribution to decrease and increase the activity respectively. It's seen that the positions 1, 2, 22, 23 of the structural skeleton (Fig.5) if positive ionic groups are present it will give negative activity.

CONCLUSION

Thus to summarize our result of the 3D QSAR model indicates it to be very predictive and statistically significant model. It may be helpful to design potent ligands in future for development of anti-trypanosomiasis drug. The structural insight will also be helpful to know about its receptor binding and bioactivity.

ACKNOWLEDGEMENT

We acknowledge AICTE for a project grant sanction under RPS for molecular modeling software.

REFERENCES

- Athri P, Wenzler T, Ruiz P, Brun R, Boykin DW, Tidwell R and Wilson WD.(2006). 3D QSAR on a library of heterocyclic diamidine derivatives with antiparasitic activity. *Bioorganic Med. Chem.* 14: 3144–3152.
- Bailly C and Chaires JB.(1998). Sequence-specific DNA minor groove binders. Design and synthesis of netropsin and distamycin analogues. *Bioconjugate Chem.* 9(5): 513-538.

- Baraldi PG, Bovero A, Fruttarolo F, Preti D, Tabrizi MA, Pavani MG and Romagnoli R.(2004).** DNA minor groove binders as potential antitumor and antimicrobial agents. *Med. Res.Rev.* 24(4): 475-528.
- Bouteille B, Oukem O, Bisser S and Dumas M.(2003).** Treatment perspectives for human African trypanosomiasis. *Fundam. Clin. Pharmacol.* 17(2): 171-181.
- Cory M, Tidwell RR and Fairley TA.(1992).** Structure and DNA binding activity of analogues of 1,5-bis(4-amidinophenoxy)pentane (pentamidine). *J. Med. Chem.* 35(3): 431-438.
- Dixon SL, Smondyrev AL, Knoll EL, Rao SN, Shaw DE and Friesner RA.(2006).** PHASE: a new engine for pharmacophore perception, 3D QSAR model development, and 3D database screening: 1. Methodology and preliminary results. *J. Comput. Aided Mol. Des.* 20(10-11): 647-671.
- Estevez AM and Simpson L.(1999).** Uridine insertion/deletion RNA editing in trypanosome mitochondria—a review. *Gene.* 240(2): 247-260.
- Fairlamb AH.(2003).** Chemotherapy of human African trypanosomiasis: current and future prospects. *Trends Parasitol.* 19(11): 488-494.
- Henderson D and Hurley LH.(1995).** *Molecular struggle for transcriptional control.* *Nature Med.* 1: 525 - 527.
- Liu B, Liu Y, Motyka SA, Agbo EE and Englund PT.(2005).** Fellowship of the rings: the replication of kinetoplast DNA. *Trends Parasitol.* 21(8): 363-369.
- Shapiro TA and Englund PT. (1990).** Selective cleavage of kinetoplast DNA minicircles promoted by antitrypanosomal drugs. *Proc. Natl. Acad. Sci.* 87(3): 950-954.
- Shapiro TA. and Englund PT. (1995).** The structure and replication of kinetoplast DNA. *Annu. Rev. Microbiol.* 49: 117-43.
- Tidwell RR and Boykin WD.(2003).** In *Small Molecule DNA and RNA Binders : From Synthesis to Nucleic Acid Complexes.* Wiley-VCH. Weinheim : Germany. p. 414-460.
- Wilson DW, Nguyen B, Tanious F, Mathis A, Hall JE, Stephans CE and Boykin DW. (2005).** Dications that target the DNA minor groove: compound design and preparation, DNA interactions, cellular distribution and biological activity. *Curr. Med. Chem. Anticancer. Agents.* 5(4): 389-408.
- Wilson DW, Tanious F, Ding D, Kumar A, Boykin WD, Colson P, Houssier C and Bailey C.(1998).** Nucleic Acid Interactions of Unfused Aromatic Cations: Evaluation of Proposed Minor-Groove, Major-Groove, and Intercalation Binding Modes. *J. Am. Chem.Soc.* 120(40): 10310-10321.
- Yeates C.(2003).** DB-289. *Immtech. Intern. Drugs.* 6(11): 1086-1093.

*Cite the article as: Banerjee S and Saikia AK.(2013). Ligand based pharmacophore modeling and QSAR analysis of heterocyclic diamidine derivatives as anti-parasitic DNA minor groove binders. *Explor.Anim.Med.Res.* 3(2): 102-116.